Laserlike Vibrational Instability in Rectifying Molecular Conductors

Jing-Tao Lü,[1,*] Per Hedegård,[2] and Mads Brandbyge[1]

[1]DTU Nanotech, Department of Micro and Nanotechnology, Technical University of Denmark, Ørsteds Plads, Building 345E, DK-2800 Kongens Lyngby, Denmark

[2]Niels Bohr Institute, Nano-Science Center, University of Copenhagen, Universitetsparken 5, 2100 Copenhagen Ø, Denmark

(Received 10 March 2011; published 20 July 2011)

We study the damping of molecular vibrations due to electron-hole pair excitations in donor-acceptor (D-A) type molecular rectifiers. At finite voltage additional nonequilibrium electron-hole pair excitations involving both electrodes become possible, and contribute to the stimulated emission and absorption of phonons. We point out a generic mechanism for D-A molecules, where the stimulated emission can dominate beyond a certain voltage due to the inverted position of the D and A quantum resonances. This leads to current-driven amplification (negative damping) of the phonons similar to laser action. We investigate the effect in realistic molecular rectifier structures using first-principles calculations.

DOI: 10.1103/PhysRevLett.107.046801 PACS numbers: 73.63.−b, 72.10.Di, 73.40.Gk, 85.65.+h

In a seminal paper from 1974, Aviram and Ratner proposed an electronic rectifier based on a single organic molecule [1]. Akin to the *p-n* junction in solid-state electronics their design involved a donor and an acceptor group bridged by a tunnel barrier (D-A). Ever since, the interest in molecule-based electronic operations, such as rectification [2–4], has increased [5]. Recently, focus has been on the interaction between the electronic current and the atomic dynamics in molecular conductors [6–8]. It is well known that a fraction of the electronic current exchange energy with the molecular vibrations leading to Joule heating [9–12]. However, instabilities such as conductance switching or breakdown occur in experiments [4,13–16] in the high voltage regime, which still poses open questions to theory. Recent theoretical work has indicated that current-induced forces can constitute an important channel of energy exchange between electrons and ions *different* from Joule heating, and lead to destabilization or runaway behavior of molecular contacts [17,18].

In this Letter we point out a generic mechanism leading to instabilities in D-A molecular rectifiers. We show that the electron-hole pair excitation by the atomic vibrations, known as electronic friction in surface science [19,20], may not necessarily damp out the vibrational energy in biased D-A molecular rectifiers. Instead, we can get negative phonon damping (friction) beyond a certain voltage. This happens when the stimulated emission of phonon dominates over absorption processes due to a population inversion, similar to what takes place in a laser.

We first outline the theoretical basis, then illustrate the effect by a simple two-level model, before presenting our first-principles calculations on realistic systems relevant for experiments.

Theory.—Within the harmonic approximation, ignoring mode-mode coupling, we can calculate the current-induced excitation of a given vibrational mode (phonon) using the rate equation approach for the phonon population N,

$$\dot{N} = \mathcal{B}(N+1) - \mathcal{A}N. \tag{1}$$

Here all phonon emission (absorption) processes are described by the rate $\mathcal{B}(\mathcal{A})$, and we have the steady-state occupation,

$$N_{\mathrm{ss}} = \frac{1}{(\mathcal{A}/\mathcal{B}) - 1}. \tag{2}$$

In equilibrium $N_{\mathrm{ss}} = n_B(\hbar\Omega)$, where n_B is the Bose occupation at the phonon energy $(\hbar\Omega)$, corresponding to $\mathcal{A} = e^{\hbar\Omega/k_BT}\mathcal{B} > \mathcal{B}$. However, out of equilibrium, when an electronic current is present, we may obtain an occupation $N_{\mathrm{ss}} \gg n_B$. Most importantly, we may obtain an instability, namely, if stimulated emission rate $\mathcal{B}$ approaches absorption rate $\mathcal{A}$. Using Fermi's golden rule, we can calculate the rates resulting from the coupling to the electronic subsystem in the presence of current,

$$\mathcal{B} = \frac{2\pi}{\hbar}\sum_{i,f}|\langle f|M|i\rangle|^2 F_i(1-F_f)\delta(\Delta\varepsilon_{fi} + \hbar\Omega). \tag{3}$$

Here M is the electron-phonon coupling, e.g., $M \propto dH/dQ$, Q being the normal mode displacement [21]. F_i and F_f are the occupation of the initial and final state, and $\Delta\varepsilon_{fi} = \varepsilon_f - \varepsilon_i$ is the energy difference between them. $\mathcal{A}$ is given by the corresponding expression with $\Omega \to -\Omega$.

For an applied voltage V, we employ the usual nonequilibrium setup with left (L) and right (R) electrodes at different chemical potential $(\mu_L - \mu_R = eV)$, corresponding to Fermi distributions n_F^α, $\alpha \in \{L, R\}$. We consider low temperatures, where $k_BT \ll eV$, $\hbar\Omega$. In

this limit $\mathcal{B}$ is only nonzero if $eV > \hbar\Omega$, and it can be written as

$$\mathcal{B} = \int_{\mu_R+\hbar\Omega}^{\mu_L} \Lambda_{LR}(\varepsilon, \varepsilon - \hbar\Omega)d\varepsilon, \tag{4}$$

introducing the electrode-resolved, coupling-weighted density of states (DOS) for the electron-hole pairs,

$$\Lambda_{\alpha\beta}(\varepsilon, \varepsilon') = \frac{1}{2\pi\hbar}\,\mathrm{Tr}[MA_\alpha(\varepsilon)MA_\beta(\varepsilon')], \tag{5}$$

given by the spectral densities A_α of scattering states originating in electrode α. In the same approximation the corresponding expression for $\mathcal{A}$ becomes

$$\mathcal{A} = \int_{\mu_R-\hbar\Omega}^{\mu_L} \Lambda_{LR}(\varepsilon, \varepsilon + \hbar\Omega)d\varepsilon + \int_{\mu_R-\hbar\Omega}^{\mu_R} \Lambda_{RR}(\varepsilon, \varepsilon + \hbar\Omega)d\varepsilon + \int_{\mu_L-\hbar\Omega}^{\mu_L} \Lambda_{LL}(\varepsilon, \varepsilon + \hbar\Omega)d\varepsilon. \tag{6}$$

We shall now assume that we are dealing with a molecule with a donor level with energy ε_D which is most strongly coupled to the left lead, while an acceptor level with energy ε_A is primarily coupled to the right lead. In this case $\Lambda_{LR}(\varepsilon, \varepsilon')$ will have a resonance as a function of ε close to ε_D and a resonance as a function of ε' around ε_A. The instability occurs when $\mathcal{B} > \mathcal{A}$. Inspecting Eq. (4), we see how $\mathcal{B}$ becomes large if ε_D is in the energy window $[\mu_R + \hbar\Omega; \mu_L]$, *and* $\varepsilon_\mathrm{D} - \hbar\Omega \approx \varepsilon_\mathrm{A}$. In this case $\mathcal{A}$ will be far from its optimum values since the integration intervals in Eq. (6) are far from the resonances of Λ_{LR}, Λ_{RR}, Λ_{LL}. The instability can also be described as the electron-hole pair damping rate [19,21],

$$\gamma^\mathrm{eh} = \mathcal{A} - \mathcal{B} \tag{7}$$

going negative. In principle other damping mechanisms such are coupling to bulk phonons, could be added to γ^eh.

Simple two-level model.—In Fig. 1(a), we consider the simplest model with a donor level ($\varepsilon_\mathrm{D} = -\varepsilon_0$) which couples with the left electrode (Γ_D), and an acceptor ($\varepsilon_\mathrm{A} = \varepsilon_0$) coupling to right electrode (Γ_A). If the DA hopping matrix element, t, is small, these levels will follow the nearby electrode chemical potential [22]. We introduce an electron-phonon coupling corresponding to modulation of the DA hopping "distance," $m \propto dt/dx$.

The processes involved at $T = 0$, are shown in Figs. 1(b)–1(d). In equilibrium ($\mu_L = \mu_R = \mu_0$) electron-hole pair generation both intra- and interelectrode lead to damping (absorption), see Fig. 1(b). The high D(A)-DOS around $\varepsilon_\mathrm{D}(\varepsilon_\mathrm{A})$ will dominate processes when both DOS peaks are within the "voltage window" $[\mu_R; \mu_L]$ and have a different filling. As the bias is increased the $\varepsilon_\mathrm{D}(\varepsilon_\mathrm{A})$ moves up (down). A maximum damping is expected when the filled D states are separated from the empty A states by $\varepsilon_\mathrm{A} - \varepsilon_\mathrm{D} \approx \hbar\Omega$ making absorption ($\mathcal{A}$) a dominating process, see Fig. 1(c). More interestingly, as the bias is further increased so $\varepsilon_\mathrm{D} - \varepsilon_\mathrm{A} \approx \hbar\Omega$ we have a situation of "population inversion": Electronic transitions from ε_D (filled) to ε_A (empty) now make phonon emission dominate over absorption, see Fig. 1(d). This corresponds to the Λ_{LR} $(\varepsilon, \varepsilon - \hbar\Omega)$ term and thus $\mathcal{B}$ to be dominating. For fixed m and sufficiently small t we reach a situation where the friction becomes negative when $\varepsilon_\mathrm{A} - \varepsilon_\mathrm{D} \approx \hbar\Omega$, Fig. 1(e). For big D-A coupling the effect disappears as the coupling makes bonding or antibonding DA states more relevant. For a particular choice of t the generic behavior of a maximum followed by negative values of γ^eh is clearly seen, Fig. 1(f).

We conclude that the negative damping $\gamma^\mathrm{eh} < 0$ is similar to the optical gain in a laser. In the presence of bias, the D state, filled by electrons, is located at an energy above the empty A state. In this case a phonon gets amplified by the stimulated emission accompanying electronic transitions from ε_D to ε_A. This is analogous to the population inversion and stimulated emission of photons in lasing: the

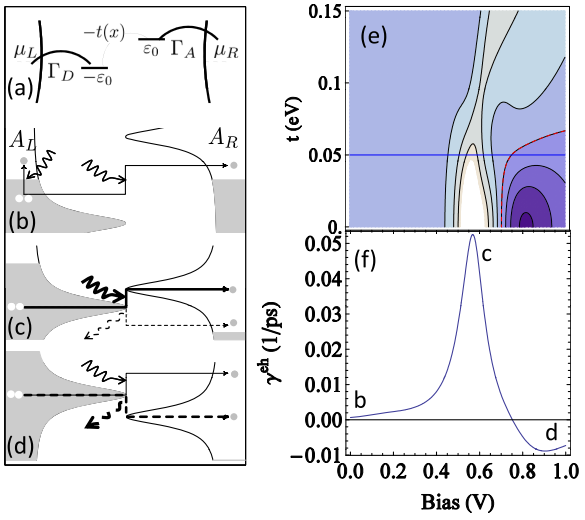

FIG. 1 (color online). (a) Simple two-level model for the donor-acceptor (DA) system. (b)–(d) D- and A-DOS and filling (gray) at $T = 0$. The D (A) levels follow the chemical potential $\mu_L(\mu_R)$ of the closest $L(R)$ electrode. (b) For zero voltage $eV \equiv \mu_L - \mu_R = 0$ only absorption processes around $\mu_L = \mu_R \equiv \mu_0$ are possible. Similar excitations from the right electrode are not shown. (c) Absorption dominates for a voltage where $\varepsilon_\mathrm{A} - \varepsilon_\mathrm{D} \approx \hbar\Omega$ and γ^eh is maximal. (d) Population inversion for larger voltage when $\varepsilon_\mathrm{D} - \varepsilon_\mathrm{A} \approx \hbar\Omega$: emission dominates and $\gamma^\mathrm{eh} < 0$. (e) Contours of $\gamma^\mathrm{eh}(V)$ for varying t (dark is negative), $\varepsilon_0 = 0.35$ eV, $\Gamma_1 = 0.3$ eV, $\Gamma_2 = 0.1$ eV, $m = 0.005$ eV, $\hbar\Omega = 20$ meV, $\mu_0 = -0.2$ eV. (f) $\gamma^\mathrm{eh}(V)$ for $t = 0.05$ eV showing the generic behavior (maximum followed by negative values).

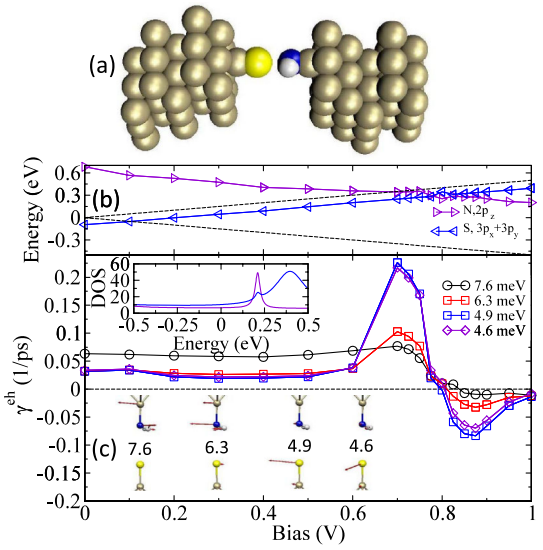

FIG. 2 (color online). (a) Molecular STM junction: S atom adsorbed on the left adatom (''tip''), the right (''sample'') adatom has adsorbed an NH_2 molecule. (b) Positions of the D ($3p_x$, $3p_y$ of S) and A levels ($2p_z$ of N) as a function of bias. The dashed lines indicate μ_L, μ_R. Inset: Left and right DOS for 1 V bias. (c) Electron-hole damping (γ^{eh}) as a function of bias for unstable phonon modes (inset) showing $\gamma^{eh} < 0$ at high bias.

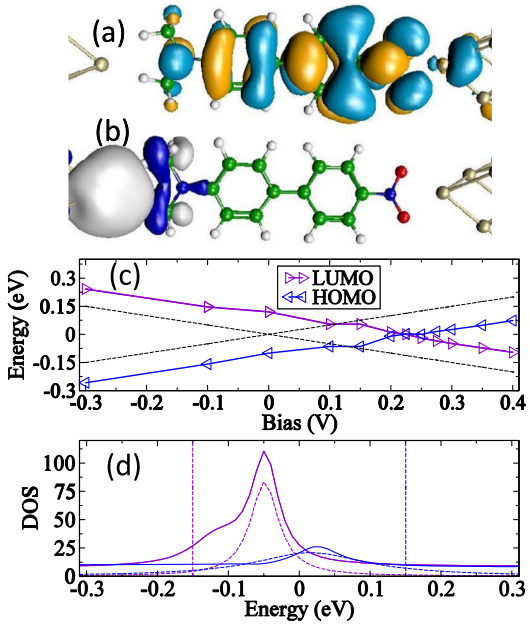

FIG. 3 (color online). (a),(b) The A (LUMO) and D (HOMO) states at 0.3 V ($\mu_L = 0.15$ V, $\mu_R = -0.15$ V shown as vertical lines). (c) The position of D and A levels (DOS peaks) as a function of bias. (d) The A_L, A_R at 0.3 V. The dashed lines include only contribution from the single D or A orbitals, while the solid lines include all contributions.

molecule is the gain material, the nonequilibrium electrons are the source, which keep pumping energy to the vibrations by stimulated emission of phonons.

First-principles calculations.—We have performed NEGF-DFT based transport calculations [23,24] on two types of experiments, where the instability appears. In the first example, we note that the tip in an STM can be functionalized by adatoms [25] or molecules [26,27] enabling control of both voltage and hopping ($\sim t$). This offers an ideal experimental test of the instability effect. In Fig. 2(a) we consider a junction formed by two gold adatoms with S and NH_2 adsorbed, representing sample and functionalized tip. The $3p_{x,y}$ orbitals of S, located just below the μ_L, serve as D and follow μ_L. The $2p_z$ orbital of N follows μ_R, and serves as A, see Fig. 2(b). In Fig. 2(c) we show the $\gamma^{eh}(V)$ for the unstable modes with negative damping (inset). The behavior is similar to the two-level model, and involves transverse adsorbate motion as selected by the symmetry of the D and A. In the next example the D-A behavior is tied to the surface anchoring groups of the 4-dimethylamino-4'-nitrobiphenyl molecule bridging Au(111) electrodes [28,29]. We identify the D, A states from the molecular projected Hamiltonian [22]. The A state [Fig. 3(a)] penetrating to the left has a π character, while the D state with s character [Fig. 3(b)] exists near the left electrode. Again A_L (A_R) mainly involves D (A) [Fig. 3(c)] tied to $\mu_L(\mu_R)$ [Fig. 3(d)], and the unstable mode displays the typical bias dependent γ^{eh}. The D, A-state symmetries imply that the mode involves transverse vibrations, see inset of Fig. 4. In Fig. 4 we show the correlation between the interelectrode damping terms (Λ_{LR}), and the electron-phonon matrix element between the D, A states, $\langle D|M|A\rangle$. It is seen that a larger matrix element leads to higher negative interelectrode damping terms.

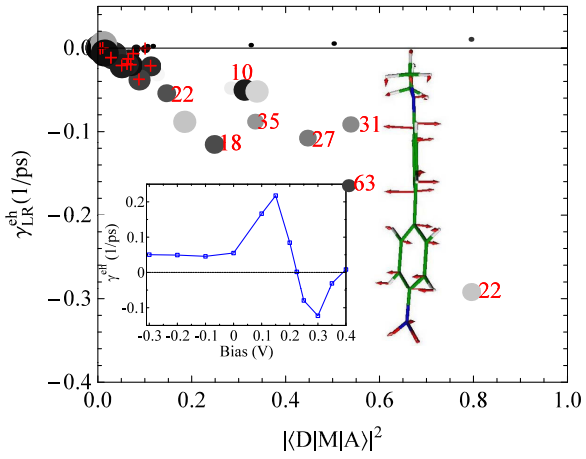

FIG. 4 (color online). Correlation between the interelectrode damping rate γ^{eh}_{LR} (including only LR terms in $\mathcal{A}$, $\mathcal{B}$), and phonon-coupling matrix element between the D and A states. Each dot represents one phonon mode. The larger dot has smaller mode frequency, and the darker one has smaller $\gamma^{eh}_{LL} + \gamma^{eh}_{RR}$. Modes displaying $\gamma^{eh} < 0$ for $V < 0.4$ V are marked with cross line or frequency. Insets: The 63 meV mode, and bias dependence of its damping rate.

Finally, we comment on the effect of other phonon damping mechanisms, e.g., due to coupling with electrode or other molecular phonons. Both of them contribute a positive damping rate. The competition of them with the mechanism proposed here eventually determines if the mode becomes unstable. If the molecule does stabilize due to these positive damping mechanisms, the high phonon occupation is still detectable in principle in the slope of the electronic differential conductance [21]. A more promising approach is to probe this occupation by Raman spectroscopy in the presence of current [10,11].

Conclusions.—We have discussed how stimulated amplification of phonons becomes possible in molecular rectifiers once the donor level is lifted higher than the acceptor by the applied bias. This is akin to population inversion leading to ''lasing,'' and may cause instabilities such as switching or contact disruption for a certain voltage [4]. Such effects require a description beyond the harmonic approximation such as molecular dynamics. On the other hand, current-induced cooling may be possible at the condition (c) in Fig. 1 [10]. Both effects draw some analog with the current-induced negative damping and cooling of a nanomechanical oscillator [30].

We thank Professor A.-P. Jauho for comments, the Lundbeck Foundation for financial support (R49-A5454), the Danish Center for Scientific Computing (DCSC) and Dir. Henriksens Fond for providing computer resources.

*jtlu@nanotech.dtu.dk

[1] A. Aviram and M. A. Ratner, Chem. Phys. Lett. **29**, 277 (1974).
[2] R. M. Metzger, Acc. Chem. Res. **32**, 950 (1999).
[3] M. Elbing *et al.*, Proc. Natl. Acad. Sci. U.S.A. **102**, 8815 (2005).
[4] I. Diez-Perez *et al.*, Nature Chem. **1**, 635 (2009).
[5] N. J. Tao, Nature Nanotech. **1**, 173 (2006).
[6] M. Galperin, M. A. Ratner, A. Nitzan, and A. Troisi, Science **319**, 1056 (2008).
[7] J. Hihath, C. Bruot, and N. J. Tao, ACS Nano **4**, 3823 (2010).
[8] N. Okabayashi *et al.*, Phys. Rev. Lett. **104**, 077801 (2010).
[9] M. Galperin, M. A. Ratner, and A. Nitzan, J. Phys. Condens. Matter **19**, 103201 (2007).
[10] Z. Ioffe *et al.*, Nature Nanotech. **3**, 727 (2008).
[11] D. R. Ward, D. A. Corley, J. M. Tour, and D. Natelson, Nature Nanotech. **6**, 33 (2011).
[12] Z. Huang *et al.*, Nature Nanotech. **2**, 698 (2007).
[13] R. H. M. Smit, C. Untiedt, and J. M. van Ruitenbeek, Nanotechnology **15**, S472 (2004).
[14] G. Schulze *et al.*, Phys. Rev. Lett. **100**, 136801 (2008).
[15] M. Tsutsui, Y. Teramae, S. Kurokawa, and A. Sakai, Appl. Phys. Lett. **89**, 163111 (2006).
[16] S. J. van der Molen and P. Liljeroth, J. Phys. Condens. Matter **22**, 133001 (2010).
[17] D. Dundas, E. J. McEniry, and T. N. Todorov, Nature Nanotech. **4**, 99 (2009).
[18] J.-T. Lü, M. Brandbyge, and P. Hedegård, Nano Lett. **10**, 1657 (2010).
[19] B. N. J. Persson and M. Persson, Surf. Sci. **97**, 609 (1980).
[20] M. Head-Gordon and J. C. Tully, J. Chem. Phys. **103**, 10137 (1995).
[21] T. Frederiksen, M. Paulsson, M. Brandbyge, and A.-P. Jauho, Phys. Rev. B **75**, 205413 (2007).
[22] K. Stokbro, J. Taylor, and M. Brandbyge, J. Am. Chem. Soc. **125**, 3674 (2003).
[23] We employ the SIESTA, TRANSIESTA/Inelastica methods [21,24], similar parameters as in Ref. [21], and the Γ-point approximation.
[24] J. M. Soler *et al.*, J. Phys. Condens. Matter **14**, 2745 (2002).
[25] L. Ruan *et al.*, Phys. Rev. Lett. **70**, 4079 (1993).
[26] T. Nishino, T. Ito, and Y. Umezawa, Proc. Natl. Acad. Sci. U.S.A. **102**, 5659 (2005).
[27] G. Schull *et al.*, Nature Nanotech. **6**, 23 (2011).
[28] M. J. Ford *et al.*, J. Phys. Condens. Matter **20**, 374106 (2008).
[29] L. A. Zotti *et al.*, Small **6**, 1529 (2010).
[30] M. P. Blencowe, J. Imbers, and A. D. Armour, New J. Phys. **7**, 236 (2005).